Minimally Invasive Therapy & Allied Technologies. Accepted for publication Jun 2018;
DOI: 10.1080/13645706.2018.1505758

A SIMPLE INSERTION TECHNIQUE TO REDUCE THE BENDING OF THIN BEVEL-POINT NEEDLES

Changhan Jun[12], Sunghwan Lim[12], Doru Petrisor[1], Gregory Chirikjian[2], Jin Seob Kim[2], Dan Stoianovici[12]

[1]Robotics Laboratory, Urology Department, [2]Mechanical Engineering Department
Johns Hopkins University, Baltimore, MD 21224, USA
Corresponding author: D. Stoianovici (dss@jhu.edu)

ABSTRACT

Objective: Needle insertion is a common component of most diagnostic and therapeutic interventions. Needles with asymmetrically sharpened points such as the bevel point are ubiquitous. Their insertion path is typically curved due to the rudder effect at the point. However, the common planned path is straight, leading to targeting errors. We present a simple technique that may substantially reduce these errors. The method was inspired by practical experience, conceived mathematically, and refined experimentally. **Methods**: Targeting errors are reduced by flipping the bevel on the opposite side (rotating the needle 180° about its axis), at a certain depth during insertion. The ratio of the flip depth to the full depth of insertion is defined as the flip depth ratio (FDR). Based on a model, FDR is constant 0.3. **Results**: Experimentally, the ratio depends on the needle diameter, 0.35 for 20Ga and 0.45 for 18Ga needles. Thinner needles should be flipped a little shallower, but never less than 0.3. **Conclusion**: Practically, a physician may expect to reduce ~80% of needle deflection errors by simply flipping the needle. The technique that may be used by hand or with guidance devices.

Keywords: Needle Insertion, Needle Deflection, Needle Steering, Needle Model

INTRODUCTION

Most image-guided diagnostic and therapeutic interventions are needle-based and accurate needle targeting is often critical for the clinical outcomes. The needle is typically aligned towards the target with the assumption that the path will remain straight during insertion (1, 2). However, this is seldom true, particularly with bevel point needles. The asymmetric surface of the bevel point acts like a rudder deflecting the path laterally on the opposite side of the bevel. Still, the large majority of needles are beveled, especially core biopsy needles. The distance between the straight and curved paths at the depth of needle insertion results in a targeting error. The error may be significant depending on the type of needle, tissues, and depth of insertion.

Using needle steering to correct for lateral path deflections is clinically relevant. But the body of research work in needle steering has focused on the opposite use, maximizing curvature in the needle path to circumvent anatomic structures; an ambition that dominates the literature perhaps due to the challenge that it poses. DiMaio, et al. proposed an ingenious method to model and simulate needle deflection due to needle tissue interaction during the insertion with finite element methods (3). Others studied the mechanical properties of biological tissues and formulated complex models of needle tissue interactions (4, 5). Park et al introduced a `unicycle' model for bevel point needle insertion (6). Webster et al introduced bicycle-like models, and experimental verification (7). They verified that bevel point needles follow a constant curvature path which depends on the properties of needle and tissue. Other groups proposed different models for bevel point needles (8, 9). Path planning and control

algorithms of theoretical needle models have also been studied for avoiding obstacles (6, 10). Overall, the most common steering application was to intentionally deflect the needle and target accurately on a curved path.

Instead, we focus on ways to maintain the needle on a straighter path. Similarly, a recent report showed that the path can be straightened by rotating the needle and using ultrasound feedback (11). Our group has also reported a method that spins the needle continuously during insertion so that the resulting helical path is straighter (12). This used a robotic system with a needle driver, similar to a drill press. We have also reported a way of maintaining the path straighter by steering the barrel of the needle from its head with a robotic system (AcuBot (13)). These straight path insertion methods required the use of devices. Other investigators proposed new needle designs for needle steering, for example a needle with a tip-articulated needle point (14). Here, we present a simple technique to be used with standard, off-the-shelf bevel pint needles, that may also be used by hand.

Physicians have previously suggested manual needle steering techniques. The most common is the trial and error under image-guidance, which involves several needle passes to reach the target (15). Cham et al. suggested a technique for lung biopsy procedures by partially withdrawing the needle and rotating it 180° before the next attempt (16). The needle flip method is not novel, being intuitively used clinically (15, 17). But this report sets a basis for the method, introduces the concept of the flip depth ratio, and gives rule-of-thumb recommendations for the physician.

We use the insertion path model of Webster et al. (7) and apply it to the manual technique of Cham et al. (16), but without withdrawing the needle. The depth flip ratio was inspired mathematically and refined experimentally.

MATERIAL AND METHODS

NEEDLE INSERTION MODEL: We used a simple needle path insertion model, called the unicycle model (6, 7). When the needle is inserted into soft tissue, a reaction force acting on the bevel surface deflects the point on the opposite side of the bevel. According to the unicycle model, the needle point trajectory is a constant radius arc. The trajectory is in the plane defined by the axis of the straight needle and the normal to the bevel surface. As such, the needle may be steered in 3D by rotating it about its axis during insertion. If the rotation is 180°, the trajectory remains within the plane but the curvature is reversed, as shown in Figure 1a. The two resulting arcs are tangent at the point where the needle was flipped. As shown in the figure, the first arc takes the point way from a straight trajectory, but the second may be used to bring it back closer. This suggests that flipping the needle at the right depth can be used to bring the point exactly on the straight trajectory at the depth of the target (Figure 1b). The aim of the study has been to investigate the depth of the flip.

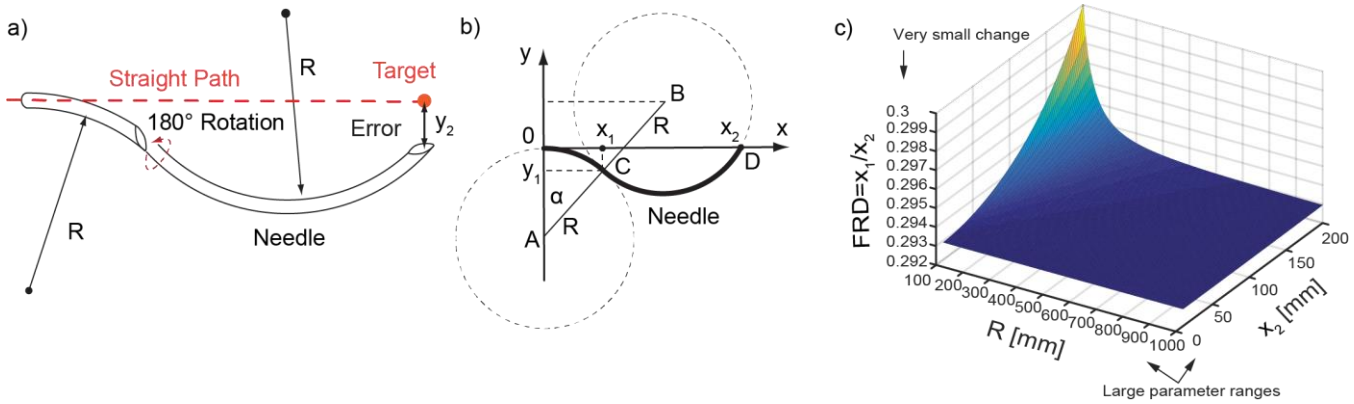

Figure 1: a) Bevel point needle inserted to a depth, rotated 180°, and inserted further, b) Needle path that returns the needle point on the straight trajectory at the depth of the target, c) The needle flip depth ratio (FDR) exhibits very little variation (0.293 - 0.300) for a wide range of its two parameters x_2 and R

In Figure 1b, insertion starts at point 0, the needle is flipped at point C, and the target is D. According to the unicycle model used, the radii of the 2 arcs are equal (AC=BC=R). For zero targeting errors the point of the needle should return to the straight path at the depth of the target (D). Previous studies (7, 11) described and modeled similar curved paths, but set their objectives differently for intended steering. The planar path of the needle that

returns onto the straight trajectory at depth x_2 after being flipped at a depth x_1 is represented in Figure 1b. The equations of the circles of the two arcs of centers A and B are:

$$x^2 + (y + R)^2 = R^2 \tag{1}$$

$$(x - 2Rsin\alpha)^2 + (y - R(2cos\alpha - 1))^2 = R^2 \tag{2}$$

The circle of center B intersects the x axis at $y = 0$. Solving (2) for x and taking the larger one of the two solutions gives:

$$x_2 = 2Rsin\alpha + R\sqrt{1 - (2cos\alpha - 1)^2} \tag{3}$$

For perfect targeting on the straight path, x_2 should coincide with the depth of the target, so x_2 is known. Then, α can be calculated from equation 3. With $\rho = x_2/2\text{R}$, $t = \tan\left(\frac{\alpha}{2}\right)$, and the half-angle formulas $\sin\alpha = \frac{2t}{1+t^2}$ and $\cos\alpha = \frac{1-t^2}{1+t^2}$

$$\rho = \frac{2t + t\sqrt{2(1 - t^2)}}{1 + t^2} \tag{4}$$

This leads to the following polynomial equation:

$$(\rho^2 + 2)t^4 - 4\rho t^3 + 2(\rho^2 + 1)t^2 - 4\rho t + \rho^2 = 0 \tag{5}$$

which yields 2 imaginary and 2 real solutions for t, of which the relevant one is the smaller one of:

$$t = \tan\left(\frac{\alpha}{2}\right) = \frac{2\rho \pm \rho\sqrt{2 - \rho^2}}{\rho^2 + 2} \tag{6}$$

This can be used to calculate α based on R and x_2.

The depth at which the needle is rotated 180° during insertion is:

$$x_1 = R\sin\alpha \tag{7}$$

We define the **Flip Depth Ratio (FDR)** as the ratio of the two depths:

$$FDR = \frac{x_1}{x_2} = \frac{Rsin\alpha}{2Rsin\alpha + R\sqrt{1 - (2\cos\alpha - 1)^2}} = \left(2 + 2\sqrt{\frac{\cos\alpha}{1 + \cos\alpha}}\right)^{-1} \tag{8}$$

Observe that, even though R has cancelled out, it is still present within α. Plugging in α makes the FDR a function of the total depth of insertion (x_2) and the radius of the path arc (R) parameters. With these, the resulting Equation 8 has a fairly complex expression (not shown). However, it is very interesting that the resulting values of the FDR exhibit very little variation on the two parameters, as shown in Figure 1c. A wide range of these parameters within practical limits is $R \in [100, 1000]$ mm and $x_2 \in [0, 200]$ mm. Still, the FDR exhibits a change of only -0.007 of 0.3, as shown in the Figure 1c.

The plateau level of the $\frac{x_1}{x_2}$ surface corresponds to small angles α, where $\cos\alpha \approx 1$. Here equation 8 is nearly constant:

$$FDR = \frac{x_1}{x_2} = \left(2 + 2\sqrt{\frac{1}{2}}\right)^{-1} = 0.293 \tag{9}$$

Results indicate that flipping the needle at a depth of approximately 0.3 of its total depth of insertion will yield nearly perfect targeting, equivalent to the straight path. According to the simple model used, this is always true, regardless of the needle, homogeneous tissue type, or needle insertion parameters. Within the limitations of the

model, the insensible variation of FDR with its included parameters suggested that **FDR may be practically constant under certain conditions.**

EXPERIMENTS: Needle insertions were performed in tissue mockups to investigate the FDR. An experimental box was built of clear polycarbonate plastic with several coaxially aligned holes on two opposite walls, as shown in Figure 2a (similar to the setup of (18)).

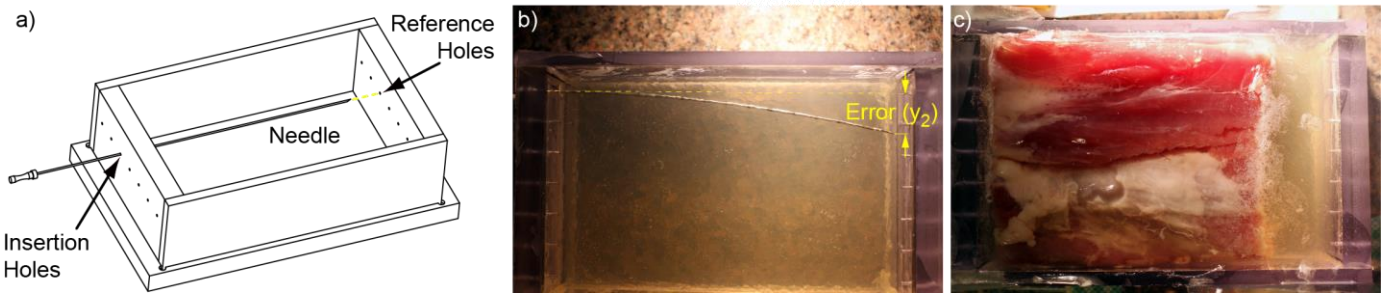

Figure 2: The setup: a) experiment box and b) targeting error measurement example, c) box with ex-vivo tissues fixed in gelatin (deepest side clear for measurements).

The size of the holes matches the gauge of the needles (18 Ga, and 20 Ga) and the walls were thick (12.7 mm) to provide a stable guide for needle insertion. The distance between the walls in the direction of needle insertion was 155 mm. The mockup consisted of the box filled with either gelatin or porcine loin fixed in gelatin. The gelatin was made of a 300 bloom gelatin powder (FX Warehouse Inc., Florida) in solution with sorbitol, glycerin, and water (3/3/2/25 parts in mass, respectively). Needles were manually inserted through the holes on one side of the box and the respective coaxial hole was used as a reference to mark the straight path, as shown in Figure 2b. The needle was inserted only once through the same hole before replacing the gelatin/tissues, to prevent following insertions to track previous paths. But multiple sets of coaxial holes (spaced 15 mm apart) were made in the same box in order to perform multiple insertions in the same experiment. Photographs of the fully inserted needle were taken and processed in Adobe Photoshop to measure the deflection error from the straight path, using the distance between the holes as a scaling reference.

The objective of the experiments was to test the theoretical 0.3 flip depth ratio, or other values hold constant in certain conditions. Logically, a FDR that yields perfect targeting always exists, but can this be predicted or approximated well enough to substantially reduce errors?

We ran experiments with two commercial (trocar) core biopsy needles of different gauges: 18Ga (d=1.270mm) x 175mm (Magnum, C.R. Bard, Covington, GA) and 20Ga (d=0.908mm) x 200mm (Achieve-Coaxial, Becton Dickenson, NJ). The bevel angle was 30° on both needles. In repeated trial and error experiments, the FDR was adjusted in order to minimize the errors. This determined the experimental values of the FDR in homogeneous matters. These were named FDR_{18Ga} and FDR_{20Ga} for the 2 needles.

To test in more realistic, less homogeneous matters the same needles were tested in porcine tissues placed in the same experiment box and embedded within the gelatin (Figure 2c). The FDR_{18Ga} and FDR_{20Ga} derived for the gelatin experiment were maintained in the tissue experiments.

Then, the 18G needle was tested in the gelatin mockup with the constant FDR_{18Ga} but different insertion depths. Furthermore, to investigate the influence of different R values, three 18G x 175mm needles (Brachystar, C.R. Bard, Covington, GA) were sharpened at the point with different bevel angles (15°, 30°, 45°). The tests were repeated with the constant FDR_{18Ga}.

Finally, additional experiments were performed to observe, understand, and try to explain why FDR may change between different gauge needles.

RESULTS

Table 1A shows the experimental results of needle insertion in gelatin with different FDR for the two needles. The lateral displacement (y_1) at the flip point (x_1) and error (y_2) at the depth of the target (x_2) are listed. Targeting

errors (y_2) without the flip (FDR=0) were large: 19.6mm (13.5% of the insertion depth x_2) for the 18Ga needle and 23.6mm (19%) for the 20Ga needle. For the 18Ga needle, targeting errors (y_2) decreased with FDR up to 0.45. For the 20Ga the errors were low at FDR 0.35 whereas errors above and below this FDR were larger. As shown by the lowest y_2 values, experimental results in gelatin suggest that FDR_{18Ga} is near **0.45** and FDR_{20Ga} is near **0.35**. The flip did not eliminate the errors, but reduced targeting errors by approximately 96% for both needles. In the following experiments the FDR was locked at these values.

Table 1B shows the results with porcine tissues for the 18Ga and 20Ga needles. Using the flip reduced targeting errors with 79% for the 18Ga needle and 87% for the 20Ga needle.

Table 1: Experimental Results

A. Needle insertion in gelatin mockup				
FDR	18_{Ga} Needle Insertion depth x_2 = 145mm		20_{Ga} Needle Insertion depth x_2 = 125mm	
	Lateral displacement (y_1) at flip point (x_1)	Targeting error (y_2) at depth of target (x_2)	Lateral displacement (y_1) at flip point (x_1)	Targeting error (y_2) at depth of target (x_2)
0.00 (No Flip)	N/A	19.6	N/A	23.6
0.30	0.6	7.16	2.7	2.6
0.35	N/R	N/R	3.3	**0.9 (96% less than No flip)**
0.40	0.8	2.5	6.5	5.12
0.45	1	**0.65 (97% less than No flip)**	7.2	5.93

N/A = Not applicable, N/R = Not required

B. Needle insertion in porcine tissue mockup				
Needle	Insertion Depth [mm]	Targeting Error (y_2) at depth of target (x_2)		
		FDR= 0 (No Flip)	FDR_{18Ga}= 0.45	FDR_{20Ga}= 0.35
18 Ga	145	9.15	**1.97 (79% less than No flip)**	—
20 Ga	125	18.59	—	**2.38 (87% less than No flip)**

C. 18Ga needle insertion in gelatin with constant FDR_{18Ga}=0.45 at different depths of insertion	
Depth x_2 [mm]	Targeting Error (y_2) at depth of target (x_2)
65	0.25
80	0.5
95	0.67
110	0.21
125	0.46
145	0.65
Average (SD)	0.46 (0.19)

D. 18Ga needle insertion in gelatin with constant FDR_{18Ga}=0.45 at 145 mm insertion depth and different bevel angles	
Needle Bevel Point Angle [°]	Error [mm]
15°	0.38
30° (typical)	0.64
45°	0.9
Average (SD)	0.64(0.21)

The results of the experiments using the same $FDR_{18Ga} = 0.45$ for different needle depths are shown in Table 1C. The errors were relatively small, 0.46mm average (SD 0.19mm), and the series of values at increasing depths (0.25, 0.5, 0.67, 0.21, 0.46, 0.65) did not suggest a dependency on the insertion depths.

Table 1C reveals the results of the experiments conducted to verify if FDR is substantially influenced by the angle of the bevel point. Targeting errors using the same $FDR_{18Ga} = 0.45$ were also small, 0.64mm avergage (SD 0.21mm) and a slight increase with the angle (0.38mm to 0.9mm).

As shown above, FDR was different for the 2 needles and for the model: $FDR_{18Ga} \approx 0.45$, $FDR_{20Ga} \approx 0.35$, and model FDR ≈ 0.3. A reasonable cause is that the simple model used does not account for the structural stiffness of the needle and the medium. The experimental values suggest that thicker needles, which bend harder, have a larger coefficient. On the other side, it appears that the theoretical method models a very thin needle.

Insertion experiments with an 18Ga needle in the gelatin mockup were performed to observe the behavior above, as much as possible. Figure 3a shows a photograph of the needle at the flip point (x_1). The lateral displacement of the needle point at the x_1 position was y_{1a}. Then, the needle was flipped and fully inserted to x_2 (Figure 3b). The lateral displacement at the same point x_1 has changed to $y_{1b} < y_{1a}$.

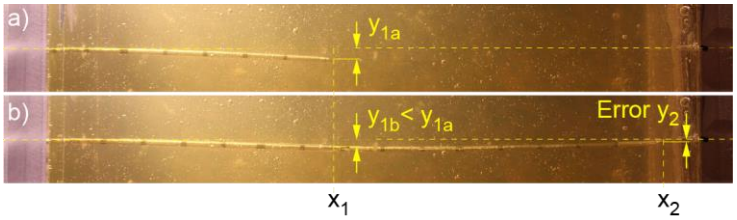

Figure 3: Two photos of an 18Ga needle inserted in gelatin:
a) at the flip position x_1, and b) at the final depth of insertion x_2.

The unicycle model considers that the trajectory of the needle is circular of a constant radius. But this is when the base of the needle is well-fixed, such as a cantilever beam. However, at the point of flipping, there is no well-fixed support. This is likely why that point moves. A possible explanation is that the elastic force of the bent needle is supported by the gelatin reaction. When the needle is flipped and inserted further, the lateral rudder force flips its direction, increasing the force that the medium should support. This reduces the displacement relative to the straight path, as shown. As such, since the displacement at the flip point is reduced after flipping, one must initially insert a little dipper before flipping, so that at the final depth the needle still returns to the straight path. This may likely explain why thicker needles have higher FDR. Since thicker needles are stiffer, their y_{12} would be smaller, so the flip point should be deeper. It is likely that the theoretical FDR value would hold well for very thin needles, so we will call this $FDR_{\infty Ga} \approx 0.3$.

It was also interesting to plot the FDR as a function of the moment of inertia of the needle cross section. Since the needles used in the study are trocar needles the cross section includes the barrel, the stylet, and a small gap in between. The moment of inertia I_y will be approximated to that of a solid round bar of the barrel outer diameter. The graph is shown in Figure 4. This has a fairly linear profile. The few experimental points used are insufficient to draw a definite conclusion, or use the curve to extrapolate other FDR values. However, since the bending stress of the needle is inversely related to I_y, the graph does not invalidate the hypothesis made above regarding the cause of the FDR change with the needle gauge.

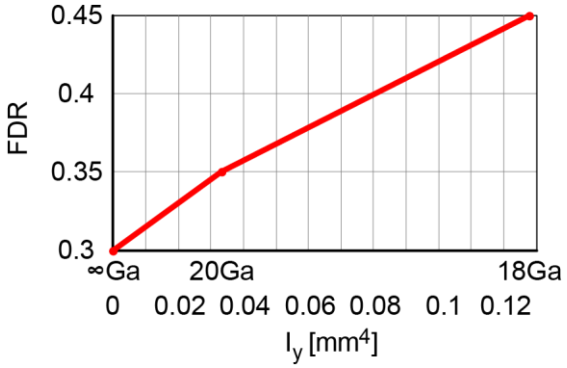

Figure 4: FDR coefficient as a function of the needle cross section moment of inertia, $I_y = \frac{\pi d^4}{64}$, where d is the needle diameter.

DISCUSSION

Needles with bevel points are ubiquitous medical instruments but notorious in their tendency to deviate from the straight path during insertion. Yet the simplest plan of needle targeting is on a straight path, and lateral deflection may cause substantial targeting errors. The technique of flipping the needle (rotating the needle about its axis with 180°) at a point during insertion has been shown to reduce the deflections in-vivo (16, 17). Here, we present the theoretical basis and in-vitro validation of the flipping method. A coefficient called Flip Depth Ratio (FDR) is introduced as the ratio of the insertion depths at which the flip is performed to the depth of the target. This gives perfect targeting according to the straight path.

Our study was called for by clinical need. In a previous study we built and tried clinically an MR Safe robot for transperineal prostate biopsy. On this path the prostate is fairly deep, on the order of 100 mm. From numerous preclinical tests, we knew that the robot orients the needle-guide on target very accurately, based on the MRI. But when 18Ga bevel needles were inserted the lateral deflections were huge, large enough to defeat the purpose of the robot assistance. We intuitively decided to flip the needle during insertion (17). At the time we did not have the results of this study, so we flipped the needle near the mid stroke, observed that this was very helpful, and this enabled us to complete the clinical trial successfully. Without the flip technique, the robot trial would have likely failed. It was this experience that prompted us to pursue the current study. Should one flip the needle at mid-stroke?

The fact that bevel needles “dive” significantly is common knowledge. The experimental results of this study confirm it, showing deflections as much as 19% of the insertion depth for the 20Ga needle.

A needle flip may be the simplest way to compensate for the lateral deflections. While most other methods require needle drivers (11-13, 19), or special needles (14), the flip can be used for standard needles, is simple enough to do by hand especially when using a needle-guide. Also, the 180° rotation keeps the trajectory within the same plane. This is beneficial if the insertion is monitored with a 2D medical imaging device, such as an ultrasound.

The theoretical model of the FDR coefficient has a complicated formula (Eq. 8 expanded with solution of α from Eq. 7). However, its value is remarkably flat on a very large range of practical parameters, FDR ≈ 0.3 (Figure 1c). Even though the model used was very simple, it pointed out that FDR may be constant for practical use. Experimentally we found that FRD depends on the needle gauge. However, it remained relatively constant for all other parameters that we investigated, different tissues, depths of insertion, and bevel angles. The vales are $FDR_{\infty Ga} \approx 0.3$, $FDR_{20Ga} \approx 0.35$ and $FDR_{18Ga} \approx 0.45$. Based on the results it appears that thicker needles that are harder to bend have a larger coefficient.

While we have experimented only with two needle gauges, these sizes are among the most commonly used clinically. Thicker needles no not normally bend, so the technique is limited to thin needles. Moreover, the experimental study was not statistically powered and the values that we found are approximate values. The exact values likely depend on numerous factors that include tissues properties and heterogeneity which are currently impossible to handle. This prompted us to keep the results in the simple form that we present herein.

CONCLUSION

The simplicity of the results makes the technique very easy to remember and apply by the physician. With an 18Ga bevel needle we recommend flipping it at about $FDR_{18Ga} \approx 0.45$ of the target depth. If the needle is 20Ga, we recommend flipping it a little shallower, at $FDR_{20Ga} \approx 0.35$. Thinner needles should be flipped a little shallower, but never less than $FDR_{\infty Ga} \approx 0.3$.

Due to numerous factors, using the technique does not eliminate targeting errors. However, the errors will be substantially reduced, and this is the simplest single thing that a physician can easily do to improve targeting. While the exact improvement cannot be predicted, experimental results in tissues suggest that errors will be reduced on the order of 80%.

ACKNOWLEDGEMENT

Some methods described in this article were supported in part by Award Number RC1EB010936 from the National Institute of Biomedical Imaging and Bioengineering. The content is solely the responsibility of the authors and does not necessarily represent the official views of the National Institute of Biomedical Imaging and Bioengineering or the National Institutes of Health.

REFERENCES

1. Cynamon J, Shabrang C, Golowa Y, Daftari A, Herman O, Jagust M: Transfemoral Transcaval Core-Needle Liver Biopsy: An Alternative to Transjugular Liver Biopsy. Journal of Vascular and Interventional Radiology. 2015.
2. Brede CM, Douville NJ, Jones J: Variable correlation of grid coordinates to core location in template prostate biopsy. Current Urology. 2012; Vol.6(4) pp.194-198.
3. DiMaio SP, Salcudean SE: Needle insertion modeling and simulation. Robotics and Automation, IEEE Transactions on. 2003; Vol.19(5) pp.864-875.
4. Okamura AM, Simone C, Leary M: Force modeling for needle insertion into soft tissue. Biomedical Engineering, IEEE Transactions on. 2004; Vol.51(10) pp.1707-1716.
5. Mahvash M, Dupont PE: Mechanics of dynamic needle insertion into a biological material. Biomedical Engineering, IEEE Transactions on. 2010; Vol.57(4) pp.934-943.
6. Park W, Kim JS, Zhou Y, Cowan NJ, Okamura AM, Chirikjian GS: Diffusion-based motion planning for a nonholonomic flexible needle model. 2005; Vol.2005 pp.4600-4605.
7. Webster RJ, Kim JS, Cowan NJ, Chirikjian GS, Okamura AM: Nonholonomic modeling of needle steering. The International Journal of Robotics Research. 2006; Vol.25(5-6) pp.509-525.
8. Glozman D, Shoham M: Image-guided robotic flexible needle steering. Robotics, IEEE Transactions on. 2007; Vol.23(3) pp.459-467.
9. Abolhassani N, Patel R, Moallem M: Needle insertion into soft tissue: A survey. Medical engineering & physics. 2007; Vol.29(4) pp.413-431.
10. Alterovitz R, Goldberg K, Okamura A: Planning for steerable bevel-tip needle insertion through 2D soft tissue with obstacles. 2005; Vol.2005 pp.1640-1645.
11. Waine M, Rossa C, Sloboda R, Usmani N, Tavakoli M: Needle Tracking and Deflection Prediction for Robot-Assisted Needle Insertion Using 2D Ultrasound Images. Journal of Medical Robotics Research. 2016; Vol.1(01) pp.1640001.
12. Badaan S, Petrisor D, Kim C, Mozer P, Mazilu D, Gruionu L, Patriciu A, Cleary K, Stoianovici D: Does needle rotation improve lesion targeting? International Journal of Medical Robotics and Computer Assisted Surgery. Jun 2011; Vol.7(2) pp.138-147. http://urobotics.urology.jhu.edu/pub/2011-badaan-ijmrcas.pdf
13. Stoianovici D, Cleary K, Patriciu A, Mazilu D, Stanimir A, Craciunoiu N, Watson V, Kavoussi LR: AcuBot: A Robot for Radiological Interventions. IEEE Transactions on Robotics and Automation. Oct 2003; Vol.19(5) pp.926-930. http://urobotics.urology.jhu.edu/pub/2003-stoianovici-ieeetra.pdf.
14. van de Berg NJ, Dankelman J, van den Dobbelsteen JJ: Endpoint Accuracy in Manual Control of a Steerable Needle. J Vasc Interv Radiol. Feb 2017; Vol.28(2) pp.276-283 e272.
15. Brown KT, Getrajdman GI, Botet JF: Clinical trial of the Bard CT guide system. Journal of Vascular and Interventional Radiology. 1995; Vol.6(3) pp.405-410.
16. Cham MD, Lane ME, Henschke CI, Yankelevitz DF: Lung biopsy: special techniques. Semin Respir Crit Care Med. Aug 2008; Vol.29(4) pp.335-349.
17. Stoianovici D, Kim C, Petrisor D, Jun C, Lim S, Ball MW, Ross AE, Macura K, Allaf ME: MR Safe Robot, FDA Clearance, Safety, and Feasibility of Prostate Biopsy Clinical Trial. IEEE-ASME Transactions on Mechatronics. 2017; Vol.22(1) pp.115-126. http://urobotics.urology.jhu.edu/pub/2017-stoianovici-tmecha.pdf

18. Blumenfeld P, Hata N, DiMaio S, Zou K, Haker S, Fichtinger G, Tempany CM: Transperineal prostate biopsy under magnetic resonance image guidance: a needle placement accuracy study. J Magn Reson Imaging. Sep 2007; Vol.26(3) pp.688-694.
19. Jun C, Kim C, Chang D, Decker R, Petrisor D, Stoianovici D: Beveled Needle Trajectory Correction. *American Urological Association, Engineering and Urology Society, 28th Annual Meeting.* 2013; pp.37. http://engineering-urology.org/am/28EUS_2013.pdf.